

Ising model with magnetic field and the lattice gas*

G. D. Mahan and Francisco H. Claro[†]

Physics Department, Indiana University, Bloomington, Indiana 47401

(Received 13 January 1977)

Approximate solutions in two and three dimensions are given for the Ising model with magnetic field, and the corresponding lattice gas. Results were obtained using nonlinear renormalization-group methods with periodic cell clusters. The two-dimensional lattices are square, honeycomb, and triangular. The three-dimensional lattices are sc, bcc, and fcc.

I. INTRODUCTION

We report numerical solutions to the Ising model with magnetic field, and to the corresponding lattice-gas model.¹ Renormalization-group techniques are used to obtain approximate solutions in two and three dimensions for a number of lattices. The two-dimensional results improve some results reported previously.² Our primary interest is in the order-disorder transformation of the lattice gas, and the corresponding ordered phase of the Ising antiferromagnet in a magnetic field.

Our basic method originates in the suggestion of Niemeyer and Van Leeuwen³ that the renormalization transformation⁴⁻⁶ proceed in real space. They divided the lattice into cells, and derived the effective interaction between cells. They used a number of concepts which have become standard, such as the multiplicity of coupling constants, eigenvalues at fixed points, and their relationship to critical exponents. They suggested a number of ways of effecting the renormalization transformation,^{7,8} but none of them work when a magnetic field is added to the Ising model.⁹

The method which does work in a magnetic field is the periodic cell-cluster transformation of Nauenberg and Nienhuis.^{10,11} They arrange the cells into clusters which are periodic in the lattice. This provides a straightforward way of evaluating the renormalization transformation. They also made the important observation that the free energy per spin could be accurately evaluated by iterating the renormalization transformation. They discussed the fixed-point structure of the square antiferromagnetic Ising model in a magnetic field.¹¹ Subbaswamy and Mahan showed how the same method could be used to solve for the corresponding lattice-gas properties.²

The above method we shall call *cell* transformations. A description of the technique of evaluating them is provided in Sec. II.

Another method, which we call a *sublattice* transformation was introduced by Schick, Walker, and Wortis^{12,13} in their treatment of the planar-triangu-

lar (pt) lattice. The lattice is divided into sublattices, typically two, three, or four. For each sublattice, a periodic arrangement of spins is taken which is called a "cell." Of course, these are not adjacent in real space, so are different than the cells of Niemeyer and Van Leeuwen. The remaining steps in the renormalization transformation are identical to the periodic cell-cluster method of Nauenberg and Nienhuis.

When comparing the two methods, cell and sublattice, each has some advantages. The cell method seems more accurate for describing ferromagnetic phase transitions. One seems to get more accurate transition temperatures, critical exponents, etc. For example, not one of the sublattice transformations we have done in two dimensions has produced a specific-heat singularity at the ferromagnetic transition. The sublattice method seems better for antiferromagnetic transitions. One can generally describe the antiferromagnetic ordering with fewer spins in the cell cluster, which eases computation. It also had the notable success of describing the antiferromagnetic phase of the pt lattice.¹² The cell method failed to do this, which is still somewhat of a mystery.²

However, the largest advantage of the sublattice method is that it works well in three dimensions, with a small number of spins. We have found by experience that practical computations are possible for about twenty spins per cluster. The number of averages one takes per transformation is 2^n , where n is approximately the number of spins per cluster. Larger clusters get unwieldy. This has prevented three-dimensional work with the cell method, since all cell-cluster arrangements seem much larger than twenty.⁸ The sublattice method works very well in three dimensions. The fcc can be done with 16 spins,¹⁴ which is just the same number previously used in the square lattice in two dimensions.^{10,11} Similarly, good results are obtained for the sc (simple cubic) and bcc lattices. Our two-dimensional results are reported in Sec. III, and the three-dimensional results in Sec. IV. Our computations are for the $S = \frac{1}{2}$ Ising model.

Position-space renormalization-group results have been recently published for the $S=1$ Ising model.^{8,15,16}

II. METHOD

We are trying to solve the Ising model with magnetic field

$$\beta H_I = -K_1 \sum_i \sigma_i - K_2 \sum_{\langle ij \rangle} \sigma_i \sigma_j, \quad (2.1)$$

where the second summation runs over nearest-neighbor pairs. The nearest-neighbor coupling constant $K_2 = \beta J$ is positive for ferromagnetic coupling and negative for antiferromagnetic coupling. We normalize all parameters by $\beta = 1/K_B T$. Thus the temperature is K_2^{-1} and the magnetic field is $K_1/K_2 = B/J$. Once we obtain the Gibbs free energy per spin

$$F_I(K_1, K_2) = (1/N) \ln(\text{Tr} e^{-\beta H}), \quad (2.2)$$

the concentration of the equivalent lattice gas is simply¹

$$C = \frac{1}{2} \left(1 + \frac{\partial}{\partial K_1} F_I(K_1, K_2) \right). \quad (2.3)$$

Our renormalization-group calculations use the nonlinear cellular method introduced by Niemeyer and Van Leeuwen.² Their method was tried of cumulant expansion^{7,8} and finite clusters, but they both gave poor results for the Ising model with magnetic field.⁹ Very good results were obtained using the periodic cluster method of Nauenberg and Nienhuis.^{10,11} We take this opportunity to describe in detail the method of periodic clusters.

In the Niemeyer and Van Leeuwen method, the renormalization proceeds in real space. The lattice is divided into cells, where each cell typically contains three to five spin sites. When the cells are chosen such that the cells form the same lattice as the original spins, this is a renormalization transformation. When the cell lattice is different than the original spin lattice, this is called a mapping. In the Ising model, the spins are denoted $\sigma_j = \pm 1$. The cell is assigned a spin $S_\alpha = \pm 1$. For an odd number of sites per cell this is usually selected to be the sign of the net cell spin

$$S_\alpha = \text{sgn} \left(\sum_{j=1}^L \sigma_j \right).$$

For an even number of sites per cell, there is some flexibility in ways of assigning site configurations to $S = -1$ or $+1$.^{15,16} Usually this is done so that the -1 configurations are the spin flip of those for $S = +1$. Figure 1 shows some of our cells for two-dimensional lattices.

If L is the number of sites per cell, then there

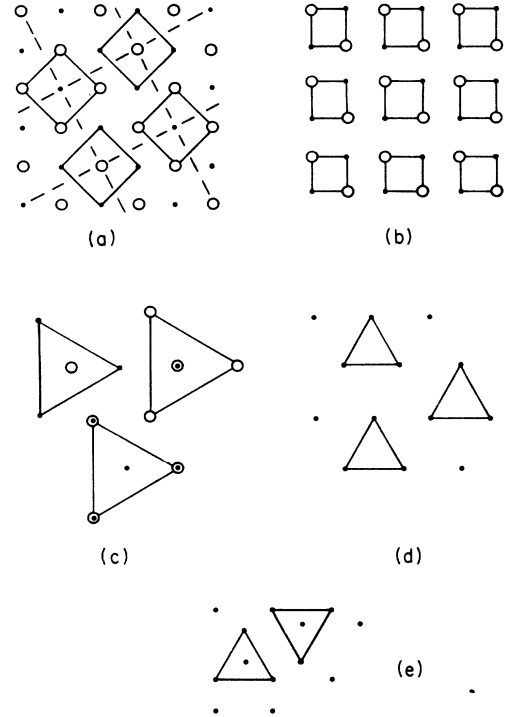


FIG. 1. Two-dimensional cell transformation: (a) 5×4 and (b) 4×4 on the sq lattice. The 5×4 transforms antiferromagnetically, while the 4×4 does not. (c) 4×3 and (d) 3×3 transformation on the pt lattice. The 4×3 transforms antiferromagnetically, but does not show a antiferromagnetic phase transition. (e) 4×2 for the hc lattice.

are 2^{L-1} configurations in a cell for each value of $S = +1$ or -1 . Call these internal configurations τ_j . The renormalization transformation is a partial summation of the trace wherein one assumes values for the S_α and then sums over all configurations τ_j consistent with these cell spins

$$f(S_1, S_2, \dots, S_{N/L}) = \text{Tr}_{\tau_j} e^{-\beta H(\sigma)}. \quad (2.4)$$

One anticipates that the interaction of cells among themselves would have the same form as the original Ising Hamiltonian, so we write

$$\ln f = -\beta H(S) = K'_1 \sum_\alpha S_\alpha + K'_2 \sum_{\langle \alpha\beta \rangle} S_\alpha S_\beta.$$

This then defines the renormalization transformation, since one can express the new coupling coefficients as functions of the original ones

$$K'_1 = W_1(K_1, K_2), \quad K'_2 = W_2(K_1, K_2).$$

However, this description is incomplete, since other interaction terms are necessary. Another problem is that one cannot, as in (2.4), actually average all N/L cells simultaneously, at least

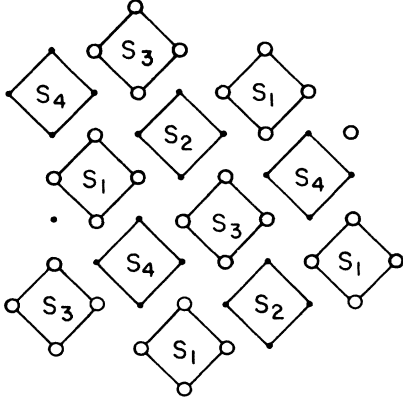


FIG. 2. Periodic cell-cluster arrangement 5×4 for the sq lattice. There are four cells per cluster, and five spins per cell.

not with present computers. So some further approximations must be introduced.

In the cluster method of Nauenberg and Nienhuis, the cells are arranged into clusters, which are assumed periodic. Alternately, one can say there is a small cluster of spins, with periodic boundary conditions. For example, Fig. 2 shows the cell periodic arrangement for a four-cell cluster. Equation (2.4) becomes simplified to

$$f(S_1, S_2, \dots, S_M) = \text{Tr}_\tau e^{-\beta H(\sigma)}, \quad (2.5)$$

where there are $2^{M(L-1)}$ configurations on the right, where M is the number of cells per cluster.

The five-site-four-cell cluster (" 5×4 ") of Fig. 2 has six distinct values for the average in (2.5): $f(1111), f(\bar{1}\bar{1}\bar{1}\bar{1}), f(\bar{1}\bar{1}11), f(\bar{1}1\bar{1}\bar{1}), f(\bar{1}\bar{1}\bar{1}1), f(\bar{1}\bar{1}\bar{1}\bar{1})$. The last two differ from the first two only when there is a magnetic field, which we are including. Thus $f(S_1, S_2, S_3, S_4)$ must be chosen so that it also generates six independent terms, or six coupling constants. This unique choice is

$$\begin{aligned} \ln f(S_1, S_2, S_3, S_4) = & a_1 K'_1 (S_1 + S_2 + S_3 + S_4) \\ & + a_2 K'_2 (S_1 + S_3)(S_2 + S_4) \\ & + a_3 K'_2 (S_1 S_3 + S_2 S_4) \\ & + a_3 K'_3 (S_2 S_3 S_4 + S_1 S_2 S_3 + S_1 S_2 S_4 + S_1 S_3 S_4) \\ & + a_4 K'_4 S_1 S_2 S_3 S_4 + a_6 G. \end{aligned} \quad (2.6)$$

The renormalized coupling parameters are K'_1 (magnetic field), K'_2 (first-neighbor pair interaction), K'_2 (second-neighbor pair), K'_3 (three spin), K'_4 (four spin), and G is the free-energy contribution. The coefficients $a_j (=1, 2, 4, 4, 4, 4)$ account for the number of times the same interaction terms occur in the periodic cluster. The coefficient of G always equals M .

The right-hand side of (2.6) contains all possible

interaction terms among four spins. It is always necessary to use this most general form in order to obtain enough independent parameters to evaluate $f(S_1, \dots, S_M)$. Thus the number of independent coupling coefficients which must be introduced into the transformation are determined by the cluster size, and is independent of L . Equation (2.6) is solved to obtain the renormalized coupling coefficients K'_α —e.g.,

$$K'_2 = (32)^{-1} \ln [f(1111)f(\bar{1}\bar{1}\bar{1}\bar{1})/f^2(\bar{1}1\bar{1}1)]. \quad (2.7)$$

The Hamiltonian that transforms into (2.6) has the same number of coupling constants (except for the first iteration) but excluding the constant term G ,

$$\begin{aligned} H(S) = & K_1 \sum S_\alpha + K_2 \sum S_\alpha S_\delta + K_2 \sum S_\alpha S_\delta \\ & + K_3 \sum S_\alpha S_\beta S_\delta + K_4 \sum S_\alpha S_\beta S_\delta S_i. \end{aligned} \quad (2.8)$$

Thus the 5×4 renormalization transformation actually takes five parameters to six

$$K'_\alpha = W_\alpha(K_6), \quad G(K^{(n)}) = U(K_6).$$

In order to solve the simple Ising problem (2.1), we start with an initial set of parameters ($K_1^{(0)}, K_2^{(0)}, 0, 0, 0$) and go through the transformation indicated in (2.5), (2.6), and (2.7). This generates the renormalized parameters ($K_1^{(1)}, K_2^{(1)}, K_3^{(1)}, K_4^{(1)}, K_5^{(1)}$). These five parameters are used as the basis of the second transformation, which then generate $K_\alpha^{(2)}$. This iteration is repeated $n \sim 30$ times. After the first iteration, the right-hand side of (2.5) contains the most general Hamiltonian (2.8) with all coupling parameters. This is a nuisance to program since there are usually a large number of three- and four-spin terms in the cluster.

Nauenberg and Nienhuis showed that the free energy per spin (2.2) can be evaluated from this iterative procedure

$$F_I(K_1^{(0)}, K_2^{(0)}) = \frac{1}{L} \sum_{n=0}^{\infty} \frac{1}{L^n} G(K_\alpha^{(n)}),$$

where G is the constant term generated in (2.6). Accuracy is assumed whenever convergence is observed in the free energy. The actual number of terms depends sensitively on the closeness to the phase boundary.

In order to study the antiferromagnetic Ising model in a magnetic field, it is necessary to have a renormalization-group transformation which takes an antiferromagnetically ordered spin lattice into an antiferromagnetically ordered cell lattice. Qualitatively wrong results are obtained if the renormalization transformation takes antiferromagnetically arranged spins into ferromagnetically arranged cells. This is because ferromagnetic ar-

rays always renormalize into ferromagnetic arrays. The qualitative error is that the ferromagnetic coupling does not have a phase transition in a magnetic field, even when there is one in the antiferromagnetic phase. Thus, to study the antiferromagnetic phase in a magnetic field, one must only use a transformation which maintains the antiferromagnetic array. For example, the 4×4 transformation Fig. 1(b) maps antiferromagnetic into ferromagnetic, and hence cannot be used to study the antiferromagnetic phase in a magnetic field. The five site cell used by either us² or Van Leeuwen¹³ does maintain the antiferromagnetic array. For all two- and three-dimensional lattices we obtain the exact result for the zero temperature critical field $K_{1c} = Z_c K_2$, where Z_c is the coordination number, and the exact free energy per spin of the ordered phase along $T=0$ axis. Also, in all cases we find no ferromagnetic transition at finite field.

One can numerically calculate anything which can be obtained from the free energy per spin. For instance, a second derivative with respect to K_2 yields the specific heat. Its singularities mark phase boundaries. A simpler method of locating antiferromagnetic phase boundaries however is to observe the flow in parameter space since at a phase boundary the flow usually changes drastically, and converges to different fixed points in the ordered or disordered phases. In fact, watching the flows is often the only way of finding a phase boundary, since sometimes the specific heat is not singular. We are, of course, solving the Ising system approximately, and critical exponents are one of the features which are calculated. Sometimes they have calculated values which do not produce specific-heat singularities. The critical index α can be obtained from the eigenvalue at the fixed point $\alpha = 2 - \ln L / \ln \lambda$ as described by Niemeyer and Van Leeuwen.³ Table I shows critical exponents for some transformations. These should be compared with exact values $\alpha = 0$, $\delta^{-1} = \frac{1}{15} = 0.067$ in two dimensions, and series results $\alpha = 0.12$ and $\delta^{-1} = 0.2$ in three dimensions.¹⁷ Four of the first six transformations do not produce specific-heat singularities since $\alpha < -1$. The fixed point can be found by an iterative procedure based upon linearizing the renormalization equations in its vicinity. This does not work for a general point on the phase boundary. So we just evaluated a grid of points, watched the flows, and reduced the grid mesh to obtain more accurate values of the phase boundaries. The phase boundary must be found accurately in order to find the lattice-gas concentration (2.3), since typically the magnetization $\partial F_I / \partial K_1$ is varying rapidly at the phase boundary.

In Table I, the above transformations are labeled

by $L \times M C$, where L is the number of spins per cell, M is the cells per cluster, and C means cell. The other method of $L \times M S$, where the last symbol denotes sublattice. This method was introduced by Schick, Walker, and Wortis. One divides the lattice into M sublattices. For each sublattice, one takes L points which form a periodic array. Compared to the cell method, (2.6) is unchanged and only the right-hand side of (2.5) is affected. Thus, this sublattice method is in practice nearly identical to the cell method. The free energy is calculated in the same way. Again the best method of locating phase boundaries is to watch the flows. Although the flows change their behavior sharply at the phase boundary, they do not often flow to a point predictable *a priori*.

One supposes that increasing the size of the cell cluster will improve the accuracy of the result. The excellent results obtained by Niemeyer and Van Leeuwen for the pt lattice, although not obtained with periodic clusters, still suggests that the cell method improves its accuracy with increased cluster size. Unfortunately, we were disappointed in our attempts to improve accuracy in the sublattice method. Our attempt in the square (sq) lattice to double M , in going from $4 \times 2 S$ to the $4 \times 4 S$, led to a worse fixed point value. On the other hand, increasing L does improve the fixed

TABLE I. Ferromagnetic transition temperatures.

	Method	K_{2c}	K_{2c} (exact)	α	δ^{-1}
pt	$3 \times 3 C^a$	0.243	0.274	-0.320	0.136
	$4 \times 3 C^a$	0.231		-0.379	0.181
	$7 \times 3 C$	0.255		-0.223	0.117
hc	$3 \times 3 S^b$	0.185		-1.134	0.375
	$4 \times 2 C^a$	0.850	0.659	-1.607	0.015
	$3 \times 2 S$	0.517		-1.231	0.148
sq	$7 \times 2 S$	0.569		-1.230	0.131
	$4 \times 4 C^c$	0.420	0.441	-0.135	0.094
	$5 \times 4 C^a$	0.406		-0.196	0.138
sc	$4 \times 2 S$	0.425		-0.6546	0.0946
	$4 \times 4 S$	0.353		-0.526	0.254
	$3 \times (4 \times 4) C$	0.216	0.222		
bcc	$4 \times 2 S$	0.361		-1.247	0.0396
	$3 \times (4 \times 4) C$	0.161	0.157		
	$4 \times 2 S$	0.212		-0.654	0.088
fcc	$8 \times 2 S$	0.152		-0.865	0.241
	$3 \times (4 \times 4) C$	0.106	0.102		
	$4 \times 4 S$	0.097		-0.1784	0.2872

^aK. R. Subbaswamy and G. D. Mahan, Phys. Rev. Lett. **37**, 642 (1976).

^bM. Schick, J. S. Walker, and M. Wortis, Phys. Lett. **A58**, 479 (1976).

^cM. Nauenberg and B. Nienhuis, Phys. Rev. Lett. **33**, 1598 (1974).

point, as we did for both the planar-honeycomb (hc) and bcc lattices.⁷

III. TWO DIMENSIONS

Some results have been reported previously using the cell transformations.² We report here further calculations using the sublattice method for the square and honeycomb lattices.

Results for the sq lattice are shown in Fig. 3, and summarized in Table I. Two sublattice transformations were calculated: 4×2 and 4×4 . The 4×2 gave excellent results. The phase boundary as a function of magnetic field and reduced temperature is shown in Fig. 3(a). These results are very similar to those reported earlier for the 5×4 cell transformation. The 4×2 only has eight spins in the cluster, so is very easy to calculate compared to the twenty spins of the 5×4 . Figure 3(b) shows the lattice gas phase boundaries. For each concentration C of atoms on the lattice, the critical temperature T_c is calculated as a function of C . The curve is symmetric about $C = \frac{1}{2}$, so only the top half is shown. Both curves predict very similar curves for the lattice gas phase boundary, and these points are close to those reported by Bienenstock and Lewis.¹⁷ The critical temperature goes to zero as a function of concentration because, as in percolation theory, long-range order can only be established if there are a critical fraction of sites occupied. Our results show this

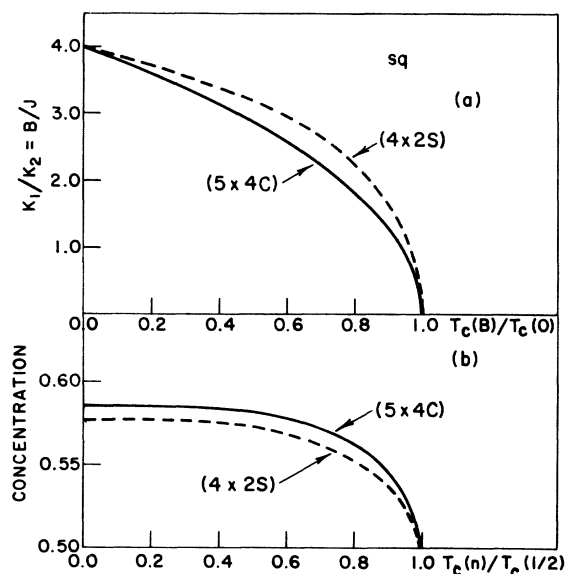


FIG. 3. Results for the sq lattice. (a) Phase boundary of Ising antiferromagnet in a magnetic field. (b) Phase boundary of the lattice gas, showing how the transition temperature varies with concentration.

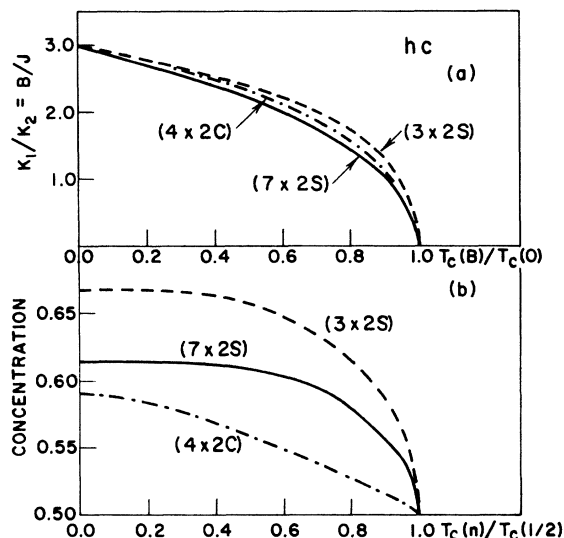


FIG. 4. Results for the hc lattice. (a) Phase boundary of Ising antiferromagnet in a magnetic field. (b) Phase boundary of the lattice gas, showing how the transition temperature varies with concentration. It is presumed that the most accurate results are the $7 \times 2S$, which has the most spins in the cluster.

critical fraction is in the range $0.42 \leq C \leq 0.58$ for the sq lattice.

Two sublattice transformations were computed for the hc lattice, 3×2 and 7×2 . These results are shown in Fig. 4, along with the 4×2 cell results reported previously. Figure 4(a) shows the phase boundary in a magnetic field for the Ising model, and all three transformations are very similar. But their lattice gas properties, shown in Fig. 4(b), are very different. The $3 \times 2S$ transformation has a critical concentration of $\frac{2}{3}$, which is identical to the value reported by Sato and Kikuchi using cluster variation methods.¹⁸ In fact, our 3×2 curve is nearly identical to theirs. The $7 \times 2S$ calculation was done to provide more accuracy, and it is supposed that this curve is closer to the correct answer.

As reported earlier the cell method does not give an antiferromagnetic phase transition for the pt lattice. This conclusion was based on the fact that the flow in parameter space for all initial values of temperature and field was towards a fixed point characterizing the disordered state. The transformations reported were the 3×3 and 4×3 . We have since performed the 7×3 transformation including 21 spins grouped in a cluster of three cells, each containing seven spins distributed over the vertices and center of a hexagon. As with the other transformations, the 7×3 was found to exhibit no antiferromagnetic transitions. In contrast, the sublattice method does give a phase boundary

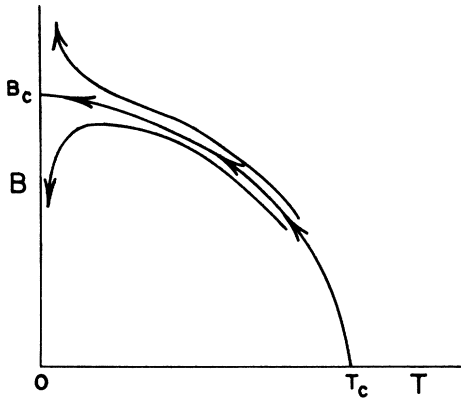


FIG. 5. Schematic drawing showing direction of flows for 7×2 S transformation of the hc lattice. If the starting point is right on the phase boundary, subsequent iterations take one to points along the boundary, with the flow towards B_c . A starting point just below the boundary also flows along the boundary, but eventually veers off towards the origin. Similarly, an initial point above the phase boundary veers off towards infinity.

marked by sharp discontinuities in the flow pattern where the boundary is located.¹² Using cell transformations one can however approximately reproduce the phase boundary so obtained by simply following specific heat maxima. We have used this method to draw the phase AB boundary for the fcc lattice, as described in Sec. IV B.

The flow pattern for the hc lattice is shown in Fig. 5. If an initial set of values $K_1^{(0)}$ and $K_2^{(0)}$ were chosen right on the phase boundary, the subsequent iterations of the renormalization transformation would describe a flow to the magnetic fixed point B_c . In practice, the initial point is not precisely on the boundary, and must be either above or below. If below, the flows follow the phase boundary, and eventually drop off and approach the origin. The point T_c is an unstable fixed point, B_c is a saddle point, and the origin is a stable fixed point. An initial point just above the phase boundary also has flows along the boundary, which eventually veer off and go to infinity. In principle, if one were to start the flows at an $\epsilon (\epsilon \rightarrow 0)$ above T_c , the flows just mark the phase boundary, and the phase boundary would be obtained in one set of iterations.

This type of flow pattern was found in all transformations with two coupling coefficients—i.e., K_1 and K_2 . Other examples are the sq, sc, and bcc. In some cases the direction of flow was reversed along the boundary, thereby approaching the point T_c . However, when one improved the calculation by increasing the number of cells, or sublattices, one also increased the number of coupling constants. Then the flows proceed in

some higher dimensional space. A simple projection back onto the K_1 and K_2 plane shows that these flows no longer followed the phase boundary in this plane.

IV. THREE DIMENSIONS

A. Cell results

No three-dimensional results have yet been reported using the cell-cluster method. The reason is simple: the smallest cluster contains too many spins, and the cluster averaging takes too long on the computer. For example, in an sc lattice one must have a minimum of eight spins per cell in order to have the cell lattice also be sc. Periodic clusters can be either two, four, or eight cells. However, only the 8×2 is few enough spins to compute conveniently. And none of these transformations is suitable for antiferromagnetic coupling since they all renormalize into a ferromagnetic phase. They are suitable for studying the ferromagnetic phase, but we have already found another method for this, which we will now describe.

If a four-spin cell is taken for an fcc lattice, in the shape of a tetrahedron as shown in Fig. 6(a), the lattice of cells is sc. If a four-spin cell is taken in the sc lattice, the resulting lattice of cells is bcc, Fig. 6(b). And a four-spin tetrahedron of the bcc lattice gives a cell lattice of fcc. Thus

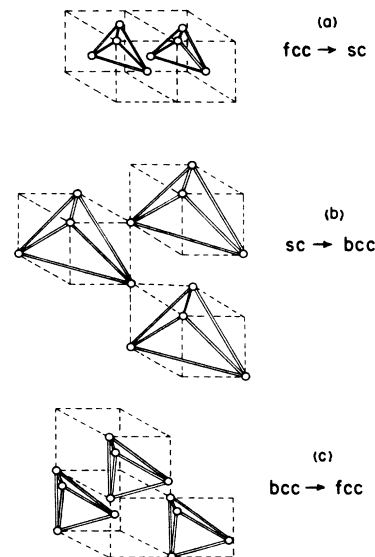


FIG. 6. Cell transformations in three dimensions. (a) tetrahedral cells of an fcc lattice produce an sc structure. (b) Tetrahedral cells in an sc lattice produce a bcc arrangement. (c) A near tetrahedral cell in bcc produces an fcc lattice. The renormalization transformation goes around the three step cycle.

the renormalization transformation can go in a cycle

$$\text{fcc} \rightarrow \text{sc} \rightarrow \text{bcc} \rightarrow \text{fcc} \rightarrow, \text{ etc.}$$

Each step of the cycle is a 4×4 , where the cluster of cells is taken in the tetrahedral arrangement of the next step in the cycle. To go around the three steps of the cycle takes 3×2^{16} spin averages, which is easily handled on the computer. In the absence of any magnetic field, the effective Hamiltonian for the sc and fcc lattices has just two terms: nearest-neighbor pair and four-spin interactions. The bcc Hamiltonian has in addition the second-neighbor-pair interaction.

The critical temperatures K_c are shown in Table I, where we compare with the exact result deduced from series expansions. The accuracy is (3–4)%. The antiferromagnetic phase, with magnetic field, cannot be studied because of the transformation maps the antiferromagnetic phase onto the ferromagnetic phase. The ferromagnetic phase does not have a phase transition in a magnetic field.

B. Sublattice results

If the sublattice method is adopted in three dimensions, then clusters with a relatively small number of spins can be conveniently chosen to treat the antiferromagnetic transition. Each lattice is first subdivided into sublattices (two of them for the sc and bcc cases, and four for the fcc case), and for each sublattice a tetrahedral arrangement of spins is chosen as the basic cell. The clusters have then two cells in the sc and bcc (thus labeled 4×2) and four cells in fcc case (4×4). We have also considered the bcc lattice

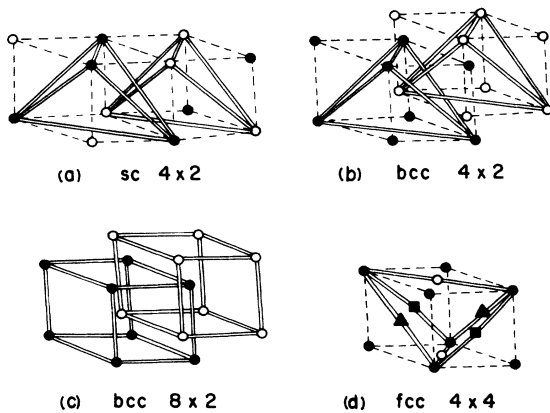


FIG. 7. Sublattice transformations in three dimensions for the sc, bcc, and fcc lattices. For the fcc, only one cell has been drawn. The other three can be obtained by displacing the tetrahedron along either face diagonal in one-half of its length.

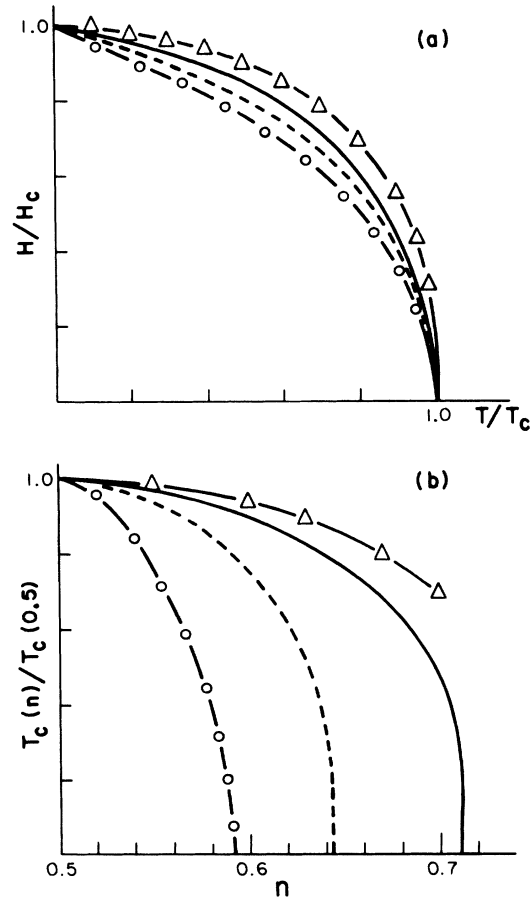


FIG. 8. Phase boundaries for the sc 4×2 (circles), bcc 4×2 (dashed lines) and bcc 8×2 (full lines) lattices. (a) Critical curve of the Ising antiferromagnet in a magnetic field. (b) Lattice gas results of critical concentration $c(T_c)$. Triangles represent the series expansion results of Bienenstock and Lewis (Ref. 10).

with an 8×2 cluster (8 spins at the corner of a cube as the basic cell, 2 cells per cluster) in order to test improvements with cell size. Unlike the cell treatment, our “cells” now only contain spins in a given sublattice, so the geometric cells may have overlapping sectors. Figure 7 shows our cell choices. It is easy to verify that in all cases an antiferromagnetically ordered lattice is transformed into a lattice of cells with the same kind of order.

Table I summarizes our results for the ferromagnetic transition. As in two dimensions, the cell method gives for the sc lattice a critical temperature value in better agreement with the high-temperature series result.¹⁹ We find however, a significant improvement if we double the number of spins per cell (8×2 result). Our critical temperature for the fcc lattice is within 5% of the comparison value almost as good an agreement as we

find for the bcc 8×2 transformation. Critical isotherm values for these two transformations are also found to agree reasonably well with the conjectured value of $\delta^{-1} = 0.2$. All of our three-dimensional sublattice transformations give a singular isothermal susceptibility at the critical ferromagnetic point.

Phase boundaries for the sc and bcc structures are shown in Fig. 8. The three lower curves in Figs. 8(a) and 8(b) are our results for the antiferromagnetic case in finite field and the lattice gas, respectively. The high temperature series results of Bienenstock and Lewis¹⁷ are also shown for comparison (triangles). Their results for the sc and bcc were identical. Agreement is again markedly improved in the bcc case with higher number of spins per cell. At finite temperatures and zero field two fixed points are found for the sc and bcc transformations, one corresponding to the ferromagnetic critical point (Table I) and the other to the antiferromagnetic transition at negative values of K_2^z .

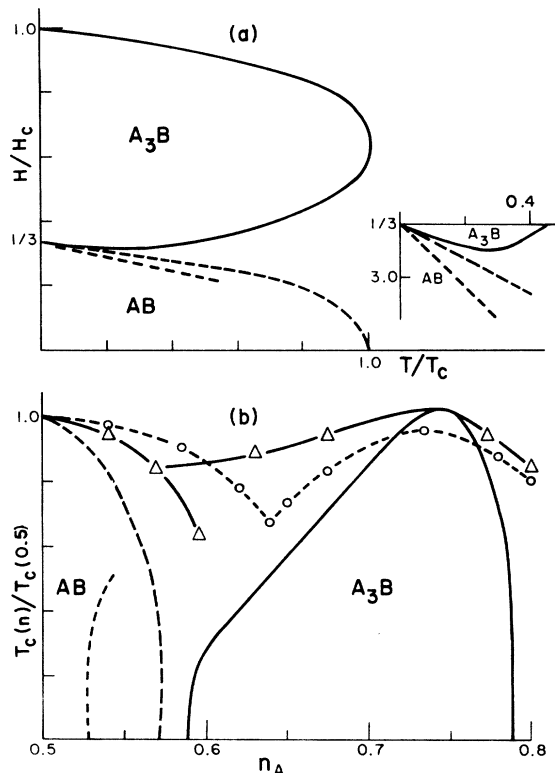


FIG. 9. Phase boundary for the fcc 4×4 lattice. (a) Critical curve of the Ising antiferromagnet in a magnetic field. (b) Lattice gas results of critical concentration. Triangles represent results of Van Baal (Ref. 20) in the Kikuchi approximation. Circles are experimental results for the Cu-Au alloy (Ref. 23). A phase boundary was found for the A_3B phase, and is shown as a solid line.

Figure 9 shows our results for the fcc lattice. Previous work²⁰⁻²² has indicated that two basic structures are expected to occur when the system becomes antiferromagnetically ordered. In one of these, three out of the four sublattices point in the direction of the magnetic field, while the fourth one points in the opposite direction. In the other, of the four sublattices two point in the opposite direction. In a binary alloy the corresponding ordered structures are the A_3B and AB , respectively. We choose the alloy for comparison with our results since we found no B - T diagram in the literature for the fcc lattice. We have then included in Fig. 9(b) the Kikuchi approximation results (Δ) for a binary alloy of Van Baal²⁰⁻²² and also experimental results (\circ) for the Cu-Au alloy.²³

Our results differ from previous work in that we found only the A_3B (and AB_3) phases were ordered. No evidence of long-range order was found for the AB phase. For the A_3B phase there were three tests for locating the phase boundary. Two of these were numerical derivatives of the calculated free energy—the specific-heat and magnetic susceptibility. Both show peaks, and the phase boundary is second order. The third test is by discontinuities in the flows. There are no fixed points or tricritical points in the K_1, K_2 , plane, except those at zero temperature. This ordered phase behaves similarly to the A_2B phase of the pt lattice found by Schick, Walker, and Wortis. There too the fixed points were at infinity. This

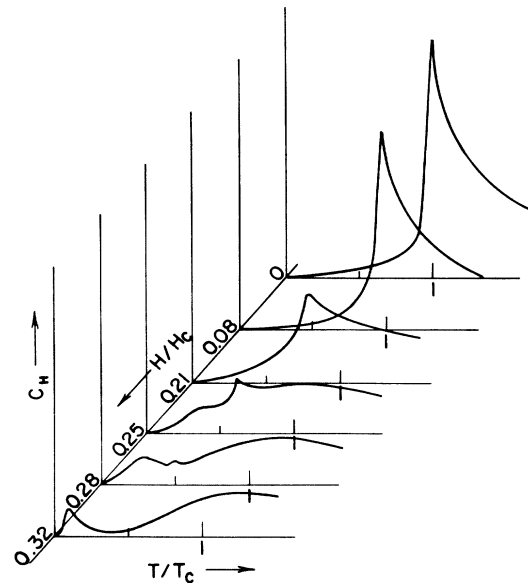


FIG. 10. Specific-heat results for the fcc lattice in the AB phase region.

phase boundary is shown as the solid line in Fig. 9.

Another remarkable feature of the A_2B phase is shown in the inset in Fig. 9(a). The phase boundary dips below the lower critical field of $4J$. For these values of constant magnetic field, two phase transitions are observed when the temperature is lowered. First, to an ordered state, and secondly back to a disordered state. This feature has not been observed in any previous work. Of course, we are not sure whether this feature is an artifact of our choice of cells and clusters, or whether it is a real feature of the fcc structure.

The dashed line in Fig. 9 delineates the region marked AB phase. We did not find a phase transition at this boundary. Rather, the dashed line denotes a locus of points where there are specific-heat maxima. These maxima are shown in detail

in Fig. 10. Near the region $H \sim 0.3H_c$ we observed two maxima, so that we show two branches of the dashed line. Careful numerical investigation revealed that these specific-heat peaks were neither singular, nor cusps, even at zero magnetic field. The susceptibility also showed rounded maxima, which were coincident with the specific-heat maxima. The flows did not show evidence of a phase boundary.

For ferromagnetic coupling, a fixed point was found at $K_1^* = 0, K_2^* = 0.09598, K_3^* = 0, K_4^* = 0.0036$.²⁴ Its exponents are shown in Table I. No similar fixed point was found on the antiferromagnetic side, at zero magnetic field. This is further compelling evidence against an actual phase transition for the AB phase. The value $K_{2c} = 0.614$ was used to normalize the axes in Fig. 9.

*Research supported by the NSF.

†Permanent address: Universidad Catolica de Chile, Santiago, Chile.

¹T. L. Hill, *Statistical Mechanics* (McGraw-Hill, New York, 1956), Chap. 7.

²K. R. Subbaswamy and G. D. Mahan, *Phys. Rev. Lett.* **37**, 642 (1976).

³T. Niemeyer and J. M. J. van Leeuwen, *Physica (Utr.)* **71**, 17 (1974); *Phys. Rev. Lett.* **31**, 1411 (1973).

⁴K. G. Wilson, *Phys. Rev. B* **4**, 3174, 3184 (1971).

⁵K. G. Wilson and J. Kogut, *Phys. Rep. C* **12**, 75 (1974).

⁶L. P. Kadanoff, A. Houghton, and M. C. Yalabik, *J. Stat. Phys.* **14**, 171 (1976).

⁷S. Hus, T. Niemeijer, and J. D. Gunton, *Phys. Rev. B* **11**, 2699 (1975).

⁸J. N. Fields and M. B. Fogel, *Physica (Utr.) A* **80**, 411 (1975).

⁹K. R. Subbaswamy, Ph. D. thesis (Indiana University, 1976) (unpublished).

¹⁰M. Nauenberg and B. Nienhuis, *Phys. Rev. Lett.* **33**, 1598 (1974); **35**, 477 (1975).

¹¹B. Nienhuis and M. Nauenberg, *Phys. Rev. B* **11**, 4152 (1975); **13**, 2021 (1976).

¹²M. Schick, J. S. Walker, and M. Wortis, *Phys. Lett. A* **58**, 479 (1976).

¹³A transformation which was partly sublattice was used by J. M. J. van Leeuwen, *Phys. Rev. Lett.* **34**, 1056 (1974).

¹⁴F. Claro and G. D. Mahan, *J. Phys. C* **10**, L73-77 (1977).

¹⁵A. Berker and M. Wortis, *Phys. Rev. B* **14**, 4946 (1976).

¹⁶T. W. Burkhardt and H. J. F. Knops, *Phys. Rev. B* **15**, 1602 (1977).

¹⁷A. Bienenstock and J. Lewis, *Phys. Rev.* **160**, 393 (1967).

¹⁸H. Sato and R. Kikuchi, *J. Chem. Phys.* **55**, 677 (1971).

¹⁹C. Domb, *Phase Transitions and Critical Phenomena*, Vol. 3, edited by C. Domb and M. S. Green (Academic, New York, 1974), p. 425.

²⁰C. M. van Baal, *Physica (Utr.)* **64**, 571-586 (1973).

²¹R. Kikuchi and H. Sato, *Acta Metall.* **22**, 1099 (1974).

²²H. Sato and R. Kikuchi, *Superionic Conductors*, edited by G. D. Mahan and W. L. Roth (Plenum, New York, 1976), pp. 135-142.

²³F. N. Rhines, W. E. Bond, and R. A. Rummel, *Trans. Am. Soc. Met.* **47**, 578 (1955).

²⁴The value of K_2^* was incorrectly given in Ref. 14 because of a typographical error.